Experimental test of modular noise propagation theory for quantum optics

Andrew G. White*, Matthew S. Taubman, Timothy C. Ralph, Ping Koy Lam, David E. McClelland, and Hans-A. Bachor
Department of Physics, Faculty of Science, The Australian National University, Australian Capital Territory 0200, Australia
(Received 27 March 1996)

We present and test against experiment a general technique that allows modular modeling of noise propagation in quantum optics experiments. Specifically, we consider a multielement frequency-doubling experiment that ultimately produces 1.7 dB/32% (3.0 dB/50% inferred) squeezing at 532 nm. Unlike previous theoretical treatments, we obtain completely analytical expressions for each element of the experiment. This allows intuitive analysis and straightforward experimental modeling. The exact role of driving noise is demonstrated: addition of a narrow linewidth mode cleaning cavity to reduce the driving noise improves the inferred squeezing from 0.75 to 3.0 dB. We find excellent agreement between the modular theory and experiment. [S1050-2947(96)07909-7]

PACS number(s): 42.50.Lc, 42.50.Dv, 42.79.Nv, 03.65.Sq

A critical but often overlooked characteristic of quantum optics experiments is their sensitivity to source noise and its effect throughout the experiment. This has implications both for practical applications, where source noise is endemic, and for modeling, which most often assumes a coherent, and thus quantum noise limited at all frequencies, source.

The best known example of a system insensitive to source noise is the squeezed vacuum produced by optical parametric oscillation. By assuming the source is a coherent state, excellent agreement has been obtained between theory and experiment [1]. This is not the case for bright squeezing produced by processes such as Kerr interactions, rate matched lasers, or second-harmonic generation. In such processes the statistics of the source beam carry over to the output beam. If the source beam is modeled as a coherent state for experiments where the source has intrinsic excess noise, the agreement between theory and experiment is quite poor [2,3].

The development of the cascaded quantum formalism [4] allowed the noise characteristics of the source to be fully modeled and propagated via a master equation approach. To date the formalism has only been explicitly tested for the case of squeezed light produced by second-harmonic generation [5]. As Fig. 1(a) shows, the system was modeled as a second-harmonic generator driven by a solid-state laser, which in turn was pumped by a coherent state. Unfortunately the cascaded formalism does not lend itself to analytical solutions, making physical interpretation of the theory difficult [6].

In this paper we present both a more elegant and complete approach and improved experimental results. The spectrum of the source, and of each subsequent element in the system, is described by completely analytical expressions, allowing both intuitive physical analysis and straightforward experimental modeling. In effect the system can be decomposed into modules, with spectra for each module being derived using the well-known technique of linearized fluctuation analysis for the equations of motion of that element [7]. The approach is general, and will predict noise spectra for any quadrature of any optical system that can be linearized. In this paper we rigorously test this approach by examining the effect of driving noise upon amplitude quadrature squeezed light produced by second-harmonic generation.

The conceptual layout of the experiment is shown in Fig. 1(b). The second-harmonic generator is driven by a laser of frequency ν_1 and produces amplitude quadrature squeezed light of frequency $2\nu_1$. The driving laser, which is in turn pumped by a diode laser, has intrinsic amplitude noise, which masks the squeezing at low frequencies [5,6]. To improve the squeezing, the laser can be passed through a narrow linewidth mode cleaning cavity, which reduces the linewidth of the amplitude noise. The full derivation of the laser spectrum is presented in Ref. [8]; the second-harmonic spectrum is a variation on the spectrum presented in Ref. [2]. Accordingly we do not repeat the derivations here, although

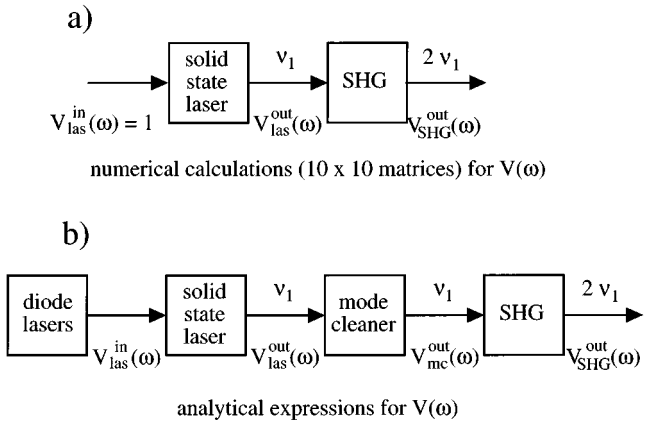

FIG. 1. Conceptual layout. (a) is the system of Ref. [5]. A second-harmonic generator (SHG) is driven by a coherently pumped laser of frequency ν_1 and produces amplitude quadrature squeezed light of frequency $2\nu_1$. Predictions are obtained via numerical calculation of large matrices. (b) is the system presented in this paper. To accurately reflect the experimental situation the solid-state laser is modeled with a noisy diode laser pump. The solid-state laser has intrinsic amplitude noise, which masks the squeezing at low frequencies: to improve the squeezing, the laser can be passed through a narrow linewidth mode cleaning cavity, which reduces the linewidth of the amplitude noise. Analytical spectra are presented for each stage of the experiment.

*Electronic address: andrew.white@anu.edu.au

we will give a brief outline of the process.

To model the noise of each element in the experiment, the quantum-mechanical equations of motion for that element are derived, including zero-point fluctuation terms (e.g., for the laser, the terms are for the pump, dipole, spontaneous emission, and cavity loss). The equations of motion are then linearized with respect to fluctuations, transformed to the frequency domain, and solved simultaneously to give the noise properties of the cavity mode a. An analytical expression V for the spectrum of the output field A is then found in terms of the mode a using the input-output formalism [9]. Explicit predictions can be made by solving the equation(s) of motion (by setting the time derivatives to zero) and substituting the subsequent semiclassical value(s) into the expression for V (e.g., for the laser, these are the values of the laser mode and populations.)

The second-harmonic generator in this experiment is singly resonant, i.e., resonant at the fundamental frequency ν_1. Accordingly we use the explicit singly resonant equation of motion [2] (as opposed to taking the limit of the doubly resonant case, cf. [6]). As we are only considering the resonant case all detunings are set to zero. Using Eq. (1a) we obtain the output amplitude quadrature noise spectrum of the second-harmonic, $V_{\mathrm{SHG}}^{\mathrm{out}}$:

$$\dot{\alpha}_{\mathrm{SHG}} = -\kappa_{\mathrm{SHG}}\alpha_{\mathrm{SHG}} - \mu|\alpha_{\mathrm{SHG}}|^2\alpha_{\mathrm{SHG}} + \sqrt{2\kappa_{shg1}}A_{\mathrm{SHG}}, \tag{1a}$$

$$V_{\mathrm{SHG}}^{\mathrm{out}} = \frac{(\mu|\alpha_{\mathrm{SHG}}|^2 - \kappa_{\mathrm{SHG}})^2 + \omega^2 + 8\kappa_{\mathrm{SHG1}}\mu|\alpha_{\mathrm{SHG}}|^2 V_{\mathrm{SHG}}^{\mathrm{in}} + 8\kappa_{shg2}\mu|\alpha_{\mathrm{SHG}}|^2}{(3\mu|\alpha_{\mathrm{SHG}}|^2 + \kappa_{\mathrm{SHG}})^2 + \omega^2}, \tag{1b}$$

where μ is the nonlinearity; the term $\mu|\alpha_{\mathrm{SHG}}|^2$ is the *two photon damping rate*, representing the nonlinear loss from the fundamental to the second-harmonic; κ_{SHG} is the total linear decay rate for the fundamental cavity; κ_{SHG1} is the decay rate of the coupling mirror; κ_{SHG2} is the decay rate due to absorptive loss and any other cavity mirrors; A_{SHG} is the driving rate; α_{SHG} is the semiclassical value of the fundamental mode; $\omega = 2\pi f$, where f is the detection frequency; and $V_{\mathrm{SHG}}^{\mathrm{in}}$ is the amplitude quadrature spectrum of the pump field. For coherent driving noise ($V_{\mathrm{SHG}}^{\mathrm{in}} = 1$), we obtain the results of Ref. 2: optimum squeezing occurs at zero frequency, and has a maximum value of 1/9 in the limit $\mu|\alpha_{\mathrm{SHG}}|^2 >> \kappa_{\mathrm{SHG}}$. If $V_{\mathrm{SHG}}^{\mathrm{in}}$ is noisy at a given frequency then the noise will mask the squeezing at that frequency, reducing its maximum value.

The mode cleaner is a way of reducing the driving noise of the second-harmonic generator, $V_{\mathrm{SHG}}^{\mathrm{in}}$. As shown in Fig. 2 the mode cleaner is a three mirror cavity with plane input and output mirrors and a curved high reflectance mirror. The equation of motion and the amplitude quadrature spectrum of the output field are straightforwardly written as

$$\dot{\alpha}_{\mathrm{mc}} = -\kappa_{\mathrm{mc}}\alpha_{\mathrm{mc}} + \sqrt{2\kappa_{\mathrm{mc1}}}A_{\mathrm{mc}}, \tag{2a}$$

$$V_{\mathrm{mc}}^{\mathrm{out}} = \frac{(2\kappa_{\mathrm{mc2}} - \kappa_{\mathrm{mc}})^2 + \omega^2 + 4\,\kappa_{\mathrm{mc1}}\kappa_{\mathrm{mc2}} V_{\mathrm{mc}}^{\mathrm{in}} + 4\,\kappa_{\mathrm{mc2}}\kappa_{\mathrm{mc}}}{\kappa_{\mathrm{mc}}^2 + \omega^2} \tag{2b}$$

where κ_{mc1} and κ_{mc2} are the decay rates for the input and output mirrors, respectively; κ_{mc}, is the total cavity decay rate, including that of the third mirror; A_{mc} is the driving rate of the cavity; α_{mc} is the semiclassical value of the mode cleaner mode; and $V_{\mathrm{mc}}^{\mathrm{in}}$ is the amplitude quadrature spectrum of the input field. At low frequencies the output spectrum is dominated by any noise due to $V_{\mathrm{mc}}^{\mathrm{in}}$. As frequency increases beyond the value κ_{mc} the ω^2 terms of both numerator and denominator become dominant, ensuring that the output becomes quantum noise limited outside the cavity linewidth. Obviously we wish to ensure that κ_{mc} is low enough so that significant noise attenuation of the input field occurs in the frequency regime of interest.

The laser is modeled as a three-level system, using the equations of motion of Ref. [8]. Rather than list these here, we present the following solutions:

$$\alpha = \sqrt{\frac{J_2(\gamma - \gamma_t)}{2\kappa} - \frac{\gamma_t}{G}}, \quad J_2 = \frac{(1 - 2\kappa/G)}{(\gamma/\Gamma + 2)}, \quad J_1 = \frac{\gamma J_2}{\Gamma},$$

$$J_3 = J_2 + \frac{2\kappa}{G}. \tag{3a}$$

The amplitude quadrature output spectrum, $V_{\mathrm{las}}^{\mathrm{out}}$ is

$$V_{\mathrm{las}} = 1 + \{(2\kappa_{\mathrm{las1}})^2[\omega^2 + (G\alpha_{\mathrm{las}}^2 + \gamma_t + \Gamma)^2] - 8\kappa_{\mathrm{las1}}\kappa_{\mathrm{las}}G\alpha_{\mathrm{las}}^2(G\alpha_{\mathrm{las}}^2 + \gamma_t + \Gamma) + 2\kappa_{\mathrm{las1}}G^2\alpha_{\mathrm{las}}^2(\Gamma J_1 V_{\mathrm{las}}^{\mathrm{in}} + \gamma_t J_3) + 2\kappa_{\mathrm{las1}}G[(\gamma_t + \Gamma)^2 + \omega^2](J_3 + J_2) + 4\kappa_{\mathrm{las1}}\kappa_{\mathrm{las2}}[(G\alpha_{\mathrm{las}}^2 + \gamma_t + \Gamma)^2 + \omega^2]\} \times \{(2G\alpha_{\mathrm{las}}^2\kappa_{\mathrm{las}} - \omega^2)^2 + \omega^2(G\alpha_{\mathrm{las}}^2 + \gamma_t + \Gamma)^2\}^{-1}, \tag{3b}$$

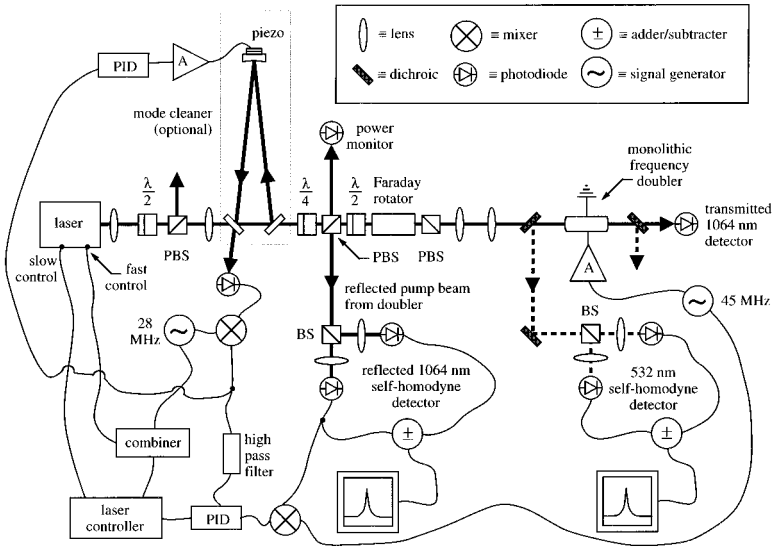

FIG. 2. Full experimental layout. The light source is a Nd:YAG monolithic ring laser (Lightwave 122) producing 200 mW of linearly polarized light at 1064 nm. The output of the laser is passed through a variable attenuator [a half-wave plate ($\lambda/2$) and polarizing beam splitter assembly] and is then incident on a three mirror, mode cleaning, ring cavity of linewidth 800 kHz. Locking of the mode cleaner is effected using a 27.650-MHz frequency modulation applied directly to the laser, and an error signal derived from the reflected light from the input mirror of the mode cleaner. At low frequencies, <500 Hz, the mode cleaner cavity length is made to track the laser frequency via a piezo on the end mirror, while at high frequencies, >500 Hz, the laser frequency is made to track the mode cleaner. The output of the mode cleaner is slightly elliptically polarized, this is corrected back to linear polarization using a zero-order quarter wave plate ($\lambda/2$). The light then passes through a Faraday isolator: this prevents light from returning to the laser, and allows easy access to the retroreflected beam. The light is then incident on the frequency-doubling cavity. Locking of the monolithic cavity is effected by placing a 45.167-MHz frequency modulation directly across the xy faces of the $MgO:LiNbO_3$ doubling cavity. The error signal is derived from the reflected beam and is used to lock the laser at both low (<500 Hz) and high frequencies to the mode of the monolith. The output second-harmonic at 532 nm is separated from the 1064-nm pump via two dichroic beam splitters. It is incident on two angled FND-100 photodetectors with retroreflectors, giving a quantum efficiency of $65\% \pm 5\%$. The outputs are added and subtracted and sent to the spectrum analyzer. BS denotes beam splitter; PBS polarizing beam splitter; PID, proportional integrator differentiator; *A* amplifier; $\lambda/2$, zero-order half-wave plate; $\lambda/4$, zero-order quarter-wave plate.

where G is the stimulated emission rate, $G=\sigma_s \rho c'$; σ_s is the stimulated emission cross section for the Nd:YAG; laser ρ is the density of Nd atoms in the laser medium; c' is the speed of light in the laser medium; γ_t and γ are the spontaneous emission rates from levels $|3\rangle$ to $|2\rangle$, and $|2\rangle$ to $|1\rangle$, respectively; Γ is the rate of incoherent pumping of the lasing transition; κ_{las1} and κ_{las2} are the cavity decay rates for the output mirror and all other losses, respectively; $\kappa_{las} = \kappa_{las1} + \kappa_{las2}$ is the total cavity decay rate; α_{las} and J_i are the semiclassical solutions for the laser mode and populations, respectively; ω is the detection frequency; and V_{las}^{in} is the amplitude quadrature spectrum of the diode laser pump field.

As can be seen from the denominator of Eq. (3b) there is a resonance in the spectrum at the frequency $\omega^2=2G\alpha_{las}^2\kappa_{las1}$. A strong oscillation, known as the resonant relaxation oscillation (RRO) [10], is apparent at this frequency if the resonance is underdamped $[2G\alpha_{las}^2\kappa_{las1} > (G\alpha_{las}^2+\gamma_t+\Gamma)^2]$. The RRO can be considered as an oscillation between photons stored in the lasing medium and photons stored in the cavity mode. Below the RRO frequency the spectrum is dominated by pump noise of the diode laser and quantum noise from the spontaneous emission and phase decay of the coherence. Above the RRO frequency these noises roll off due to the filtering effect of the lasing cavity, so that at high frequencies the laser approaches the quantum noise limit. It is the tail of the large noise feature due to the RRO that we wish to attenuate with the mode cleaning cavity.

The three equations (1b), (2b), and (3b) are straightforwardly combined to give the output squeezing spectrum of the full system. Compare this to the standard technique [11,5], which in general requires laborious numerical clacu-lations. Furthermore, modeling removal of the mode cleaner is trivial: the term V_{mc}^{out} [in the position V_{SHG}^{in} of Eq. (1b)] is replaced by V_{las}^{out}.

The experimental layout is shown in Fig. 2. The laser is a diode pumped Nd:YAG monolithic ring laser (Lightwave 122) that produces a single mode of wavelength 1064 nm. The mode cleaner is a three mirror ring cavity with a perimeter of 2.5 m. A ring cavity was chosen to allow easy access to the reflected beam, which provides the locking signal in a Pound-Drever configuration. The necessary phase modulation is achieved by modulating the fast frequency control port of the laser [12] at a frequency of 27.650 MHz. Low-frequency locking is achieved by feeding the resultant error signal to the piezo on the third mirror. Due to the narrow linewidth of the mode cleaner, this alone is inadequate for locking: high-frequency (>500 kHz) locking is effected by filtering the error signal, combining it with the 27.650-MHz modulation, and feeding it to the fast control of the laser.

The normal application of mode cleaning cavities in quantum optics requires very narrow linewidths and output pow-

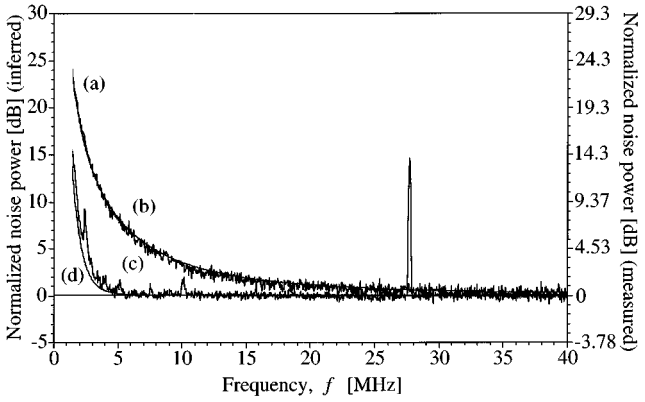

FIG. 3. A comparison of the mode cleaner and laser output spectra for power incident on the infrared balanced detector of 14 mW. The experimental traces have been corrected for electronic noise. The upper traces (a) and (b) are, respectively, the experimental and theoretical traces for the output spectrum of the laser (with the noise eater turned off). The lower traces (c) and (d) are the equivalent for the mode cleaner output spectrum. The noise filtering action of the mode cleaner is very clear. While the laser is not quantum noise limited until beyond 45 MHz, the output of the mode cleaner is quantum noise limited beyond 7 MHz. The large peak at 27.6 MHz is the modulation signal for the locking of the mode cleaner.

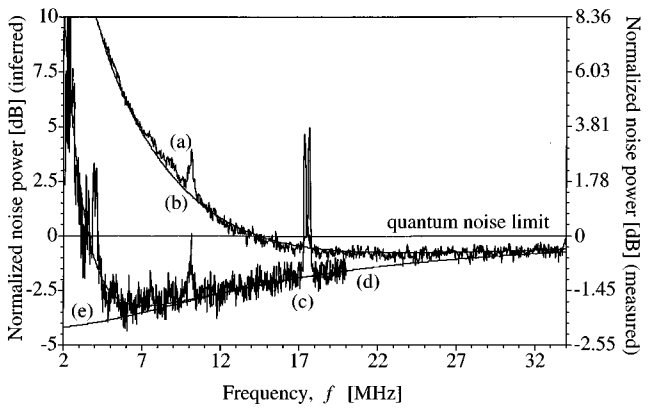

FIG. 4. Squeezing spectra of the second-harmonic. The mode matched power of the fundamental was 81 mW, the second-harmonic power was 34 mW. The experimental traces have been corrected for electronic noise. Trace (a) and trace (c) are the spectra obtained for the experiment run without and with the mode cleaner, respectively. The maximum squeezing and detection frequency of occurrence in each case are: trace (a), 0.47 dB (0.75 dB inferred) at 23 MHz; trace (c), 1.7 dB (3.0 dB inferred) at 7.5 MHz. The sub-shot noise noise feature at 10 MHz on trace (c) is residual noise from the locking systems of the mode cleaner and the second-harmonic generator. Traces (b) and (d) are the theoretical plots corresponding to the experimental traces. Trace (e) is the theoretical prediction for the squeezing if there were no extra noise present at all, i.e., the driving field was coherent.

ers of only a few mW [13]. This is achieved by designing for as high a finesse as possible, using high-reflectance coupling mirrors and lengthy perimeters. A constraint of our application is the requirement for the transmission of high powers, in excess of 100 mW. This limits the finesse, as the intracavity powers rapidly approach the damage threshold of commercially available mirrors. Accordingly we settled on input and output couplers of reflectivity 98%, and reflectivity of 99.9% for the third mirror. The cavity thus has a linewidth of 800 kHz and transmits 60% of the incident power, which is adequate for this experiment.

The decay rate for a mirror is related to the mirror reflectivity by the relation

$$\kappa \simeq \frac{c(1-\sqrt{R})}{np}, \tag{4}$$

where c is the speed of light *in vacuo* ; p is the cavity perimeter; n is the refractive index in the cavity; and R is the reflectivity of the mirror. The relationship between the driving rate of a cavity A and the power of the driving field P is $P=h\nu A^2$, where h is Planck's constant.

The values of the laser parameters for Nd:YAG are $\sigma_s=6.5\times10^{-23}\mathrm{m}^2$; $\rho=1.38\times10^{26}$atoms. m^{-3}; $c'=1.640\times10^8\mathrm{m\,s}^{-1}$; $\gamma_t=4.3\times10^3\ \mathrm{s}^{-1}$; $\gamma=3.3\times10^7\mathrm{s}^{-1}$ [14], thus $G=1.4710^{12}\ \mathrm{s}^{-1}$. Our laser has a geometric perimeter of $p=28.5$ mm, an input coupler of reflectivity $R=96.8\%$, and internal round trip losses of 1.6%. Thus $\kappa_{\mathrm{las1}}=9.28\times10^7\ \mathrm{s}^{-1}$ and $\kappa_{\mathrm{las}}=1.39\times10^8\ \mathrm{s}^{-1}$. Γ is the only fit parameter required; its value is determined by fitting the frequency of the predicted RRO to that of the experimental observed RRO. For our laser we find $\Gamma=8.703\ \mathrm{s}^{-1}$. The diode laser arrays used to pump the Nd:YAG laser suffer large, very broadband, amplitude noise. We model the diode laser spectrum as white noise 52 dB above shot noise, i.e., $V_{\mathrm{las}}^{\mathrm{in}}\simeq160\,000$. This is consistent with the directly measured noise power for diode arrays.

Light-wave lasers have a switchable internal noise eater, i.e., an optoelectronic feedback circuit that reduces the peak noise power of the RRO. Unfortunately the noise eater increases the noise in the tail of the RRO, in the frequency regime that we seek to quieten. Accordingly all data in this paper have been taken with the noise eater turned off. Figure 3 shows, at the same optical power, the output spectra of the laser and mode cleaner and the predictions from Eqs. (3b) and (2b). We note two things. Firstly, the agreement between theory and experiment is excellent. Secondly, the noise filtering action of the mode cleaner is very clear. At these powers the laser is not quantum noise limited (<0.25 dB) until beyond 45 MHz, whereas the mode cleaner output is quantum noise limited from 7 MHz onwards.

The second-harmonic generator is a standing-wave monolithic cavity fabricated from MgO:$LiNbO_3$ with dimensions of $5(x)\times12.5(y)\times5(z)$ mm, where (z) is the optic axis. The cavity ends have radii of curvature of 14.24 mm (the waist is thus 32.8 μm). The front and back ends are coated with dual wavelength dielectric mirror coatings: 99.60% $\pm$ 0.03% at 1064 nm and $\sim$ 4% at 532 nm for the front coating; 99.90% $\pm$ 0.03% at 1064 nm and 99.9% at 532 nm for the back coating. The internal round-trip losses are estimated to be $0.10\pm0.02\%\ \mathrm{cm}^{-1}$ and the nonlinearity is inferred to be $\mu=0.012\ \mathrm{s}^{-1}$. The xy faces of the crystal are gold coated to allow electro-optic modulation of the cavity. The cavity is electrically insulated inside a Teflon case that is resident in a copper oven that is temperature locked to a stability of 1 mK. The cavity is electro-optically modulated at 45.167 MHz to

produce a Pound-Drever error signal that is detected on the reflected beam accessed by the Faraday isolator. As the laser is locked to both the second-harmonic generator and the mode cleaner considerable care must be taken to ensure that there is no conflict between the locking loops. Significantly lower bandwidth mode cleaners than that used here would give only a relatively small increase in squeezing and would be much more difficult to lock: an extra degree of freedom would be required, possibly by using a hemilithic (one mirror external to the crystal) frequency-doubling cavity.

The second-harmonic generator produces squeezed light at 532 nm, which is picked off with a dichroic and detected via a self-homodyne detector. In general the quantum efficiency of available photodetectors is lower in the green than in the infrared. To maximize quantum efficiency, the photodetectors (EG&G FND-100) have the external glass removed, are turned to the Brewster angle, and the reflected light is directed back onto the detector via a curved retroreflector. These measures push the quantum efficiency of each detector to $65\% \pm 5\%$.

The second-harmonic generator was pumped with a mode-matched power of 81 mW, producing 34 mW of second-harmonic light. Higher pump powers than this cause the onset of parasitic parametric oscillation, which degrades the squeezing [15]. Figure 4 clearly shows the effect of driving noise on the squeezing of the second-harmonic. Traces (a) and (c) are the experimental spectra from the second-harmonic generator, respectively, without and with the mode cleaner. Traces (b) and (d) are the corresponding theoretical predictions. Again, the agreement between theory and experiment is excellent. Trace (e) is the theoretical prediction for a coherent pump. Comparison of trace (e) with traces (a) and (c) clearly demonstrates the role of the mode cleaner in attenuating the driving noise. The maximum squeezing is improved from 0.47 dB (0.75 dB inferred) at 23 MHz to 1.6 dB (3.0 dB inferred) at 7.5 MHz, and the spectrum above 11 MHz is that predicted for the ideal case with no excess pump noise. The subshot noise feature at $\simeq 10$ MHz is residual noise from the locking system (cf. Fig. 3).

The squeezing measurement is a sensitive test of our model. For example, the diode lasers that pump the solid-state laser have considerable excess noise (52 dB above the quantum noise limit). Despite this, excellent agreement was obtained between theory and experiment, both without the mode cleaner and in Ref. 5, by modeling the diode laser noise as quantum noise limited. This is no longer true for the mode cleaner case, where there is a greater degree of squeezing. The approximation that the diode laser pump is quantum noise limited gives poor agreement between theory and experiment: it is necessary to include the correct amount of excess classical noise.

To reiterate our earlier point: the only changes to the model between producing traces (b) and (d) was the inclusion of the mode cleaner [Eq. (2b)] at the appropriate place in Eq. (1b), and an adjustment of the parameter representing the optical power reaching the monolith. All other parameters remain fixed. The excellent agreement between theory and experiment, and the inclusion of the mode cleaner, which led to the large observed improvement in squeezing (from 0.75 to 3.0 dB, inferred), suggests a significant improvement is possible in the system of Ref. [3]. The modular approach can be applied to any experiment where transfer of source noise is significant, notably injection locked laser systems [8] and holds great potential for modeling complicated multielement experiments, such as gravity wave interferometers.

Note added in proof: Recently, we constructed photodetectors with a quantum efficiency of 91% at 532 (nm), capable of handling up to 20 mW per detector. For squeezing of 2.6 dB we have observed 2.1 dB experimentally (without correcting for electronic noise).

The authors wish to acknowledge useful discussions with Charles C. Harb. The crystal was cut and polished by CSIRO, Sydney, Australia. The mirror coatings were produced by LZH, Hannover, Germany. This work was supported by the Australian Research Council.

[1] E. S. Polzik, J. C. Carri, and H. J. Kimble, Phys. Rev. Lett. **68** 3020 (1992).

[2] R. Paschotta, M. Collett, P. Kürz, K. Fiedler, H.-A. Bachor, and J. Mlynek, Phys. Rev. Lett. **72**, 3807 (1994).

[3] H. Tsuchida, Opt. Lett. **20**, 2240 (1995).

[4] C. W. Gardiner, Phys. Rev. Lett. **70** 2269 (1993); H. J. Carmichael, *ibid.* **70**, 2273 (1993).

[5] T. C. Ralph, M. S. Taubman, A. G. White, D. E. McClelland, and H.-A. Bachor, Opt. Lett. **20**, 1316 (1995).

[6] A. G. White, T. C. Ralph, and H.-A. Bachor, J. Opt. Soc. Am. B **31**, 1337 (1996).

[7] See, for examples C. W. Gardiner, *Quantum Noise* (Springer-Verlag, Berlin, 1991); L. Hilico, J. M. Courty, C. Fabre, E. Giacobino, I. Abram, and J. L. Oudar, Appl. Phys. B **55**, 202 (1992).

[8] T. C. Ralph, C. C. Harb, and H.-A. Bachor, Phys. Rev. A (to be published).

[9] C. W. Gardiner and M. J. Collett, Phys. Rev. A **31** 3761 (1985).

[10] For example, see A. Yariv, *Quantum Electronics* (John Wiley, Singapore, 1989).

[11] D. F. Walls and G. J. Milburn, *Quantum Optics* (Springer-Verlag, New York, 1994).

[12] G. Cantatore, F. Della Valle, E. Milotti, P. Pace, E. Zavattini, E. Polacco, F. Perrone, C. Rizzo, G. Zavattini, and G. Ruoso, Rev. Sci. Instrum. **66**, 2785 (1995).

[13] G. Breitenbach, T. Muller, S. F. Pereira, J.-Ph. Poizat. S. Schiller, and J. Mlynek, J. Opt. Soc. Am. B **12**, 2304 (1995).

[14] W. Koechner, *Solid State Laser Engineering* (Springer-Verlag, Berlin, 1988).

[15] A. G. White, P. K. Lam, M. S. Taubman, T. C. Ralph, S. Schiller, D. E. McClelland, and H.-A. Bachor, in Proceedings of the Centre de Physique des Houches $\chi^{(2)}$ Workshop [J. Quantum Semiclass. Opt. (to be published)].